Key Engineering Materials
ISSN: 1662-9795, Vol. 926, pp 1457-1467
doi:10.4028/p-5fxp53

Submitted: 2021-11-29
Revised: 2022-01-21
Accepted: 2022-02-10
Online: 2022-07-22

In-Mold-Assembly of Hybrid Bending Structures by Compression Molding

Tim Stallmeister[1,a*], Thomas Tröster[1,b]

[1]Paderborn University, Chair of Automotive Lightweight Design,
Warburger Str. 100, 33098 Paderborn

[a]tim.stallmeister@upb.de, [b]thomas.troester@upb.de

Keywords: compression molding, process development, hybrid structure, lightweight design

Abstract. The further development of in-mold-assembly (IMA) technologies for structural hybrid components is of great importance for increasing the economic efficiency and thus the application potential. This paper presents an innovative IMA process concept for the manufacturing of bending loaded hybrid components consisting of two outer metal belts and an inner core structure made of glass mat reinforced thermoplastic (GMT). In this process, the core structure, which is provided with stiffening ribs and functional elements, is formed and joined to two metal belts in one single step. For experimental validation of the concept, the development of a prototypic molding tool and the manufacturing of hybrid beams including process parameters are described. Three-point bending tests and optical measurement technologies are used to characterize the failure behavior and mechanical properties of the produced hybrid beams. It was found that the innovative IMA process enables the manufacturing of hybrid components with high energy absorption and low weight in one step. The mass-specific energy absorption is increased by 693 % compared to pure GMT beams.

Introduction

Hybrid structures made of metal and fiber-reinforced plastic (FRP) exhibit lightweight potential due to the combination of high mechanical properties and low density. Such multi-material designs are used in structural applications to reduce the overall mass and increase functionality through integrative approaches. To be used in large-scale application (e. g. automotive), economic requirements such as low production costs and cycle times must be met. Therefore, glass-fiber reinforced thermoplastics are often used, as they provide low material costs and fast manufacturability. Furthermore, the unproblematic recycling of thermoplastic matrices in comparison to thermosets is an important factor for sustainable developments. [1]

State of the art. Numerous joining strategies for metal and FRP exist and can be classified into post- (PMA) and in-mold-assembly (IMA) processes. The separation of forming and assembly with PMA offers a high degree of design freedom for metal and plastic components and enables common joining processes such as adhesive bonding or mechanical joining techniques. Drawbacks of PMA are the additional handling and joining operations, which limit rationalization and automation of the production. In comparison, IMA processes offer a reduced number of manufacturing steps and lower cycle times, leading to economic benefits. [2]

Based on recent research and development activities, a trend towards further development of IMA processes can be identified [1]. The objective is to enable IMA processes for the integrated manufacturing of complex and highly functionalized hybrid structures.

One of the first IMA processes used is the injection molding of (fiber-reinforced) plastic onto metal sheet structures [3]. Thin-walled plastic ribs serve as stiffening elements to stabilize the metal against buckling under pressure load [4]. Furthermore, the plastic can contain functional elements such as bosses, tabs or snap-fittings and connect several metal sheets to each other to simplify assembly processes. The plastic flows around the metal component at openings, edges and recesses and thus achieves a macroscopic interlock of the two materials.

Ehrenstein et al. investigated the influence of coating the metal with bonding agents and plasma pretreatment of the plastic during overmolding process [5]. Therefore, a u-shaped metal sheet

component was formed and transferred into the mold where the injection of the FRP ribs took place. The investigations resulted in an increase of bending and torsion properties of the hybrid structure, which was attributed to the combined form fit and increased adhesion.

Hoffmann et al. achieved higher joint strengths between metal sheets and molded-on rib structures by laser pre-treatment of the metal surfaces [6]. The increase in strength was referred to a microscopic interlock at the undercut structures generated by the laser pre-treatment of the metal sheets. Comparable bending and torsion tests to the investigations of Ehrenstein et al. [5] were carried out on a hybrid beam that consists of two aluminum sheets and a FRP rib structure in between, that was produced by injection molding.

The mechanical properties of injection molded FRPs are limited because considerable fiber damage occurs in the manufacturing process. Shear-induced fiber breakage leads to reduced fiber lengths, which in turn reduces both the stiffness and the strength of the FRP [7]. Higher fiber length and thus better parts' performance can be achieved with compression molding [8]. Common material groups for compression processes are organosheets or glass-mat reinforced thermoplastics (GMT).

Modler et al. developed a process called 3D-hybrid that combines the forming and joining of stacked metal and organosheets via compression molding with an additional injection molding of LFT ribs [9]. The adhesion between the steel and organosheet is promoted by an epoxy-based adhesive film that is applied to the steel surface prior to forming and joining. After forming the stacked metal and organosheets the injection molding takes place in the combined forming and molding tool. Carrying out three-point bending tests resulted in 44 % higher mass-specific energy absorption of the 3D-hybrid part in comparison to a reference part that is exclusively made of steel. Furthermore, a positive effect of an additional closing plate was found out. This steel closing plate was connected to the 3D-hybrid-part by spotwelding and increased the mass-specific energy absorption by 107 %.

Fang et al. combined the forming and joining of a metal sheet and LFT rib structure by compression molding [10]. A metal sheet with applied melt adhesive and an extruded LFT compound are transferred together into a compression tool. The simultaneous deep drawing and compression molding could be achieved by using the pressure of the LFT compound to form the metal sheet. Besides the optimization of the sealing technique and process parameters, mechanical tests were carried out to analyze the parts' performance. The researchers came to the similar conclusion as Modler et al. that an additional metal sheet, joined in a second process step with the hybrid structure leads to highest mechanical properties [11].

Innovative molding technology. Considering the results of Modler et al. and Fang et al., hybrid structures exhibit highest bending properties with two metal sheets that are connected and distanced with an inner FRP rib structure. In order to substitute the additional joining process for the second metal sheet (closing plate), the innovative molding technology directly forms a glass-mat reinforced thermoplastic (GMT) rib structure and joins it between the metal sheets. Therefore, two metal sheets are vertically placed and fixed in a molding tool with vacuum (Fig. 1, a). Hot and plasticized GMT is then transferred in the cavity and between the metal sheets (Fig. 1, b). By closing the molding tool, the punch forms the rib structure and presses the GMT onto the metal sheet surfaces (Fig. 1, c). With the help of adhesive films priorly applied to the metal sheets, a surface bonding is achieved under pressure and temperature. Thus, the forming and joining of the hybrid structure is integrated in the single-step process.

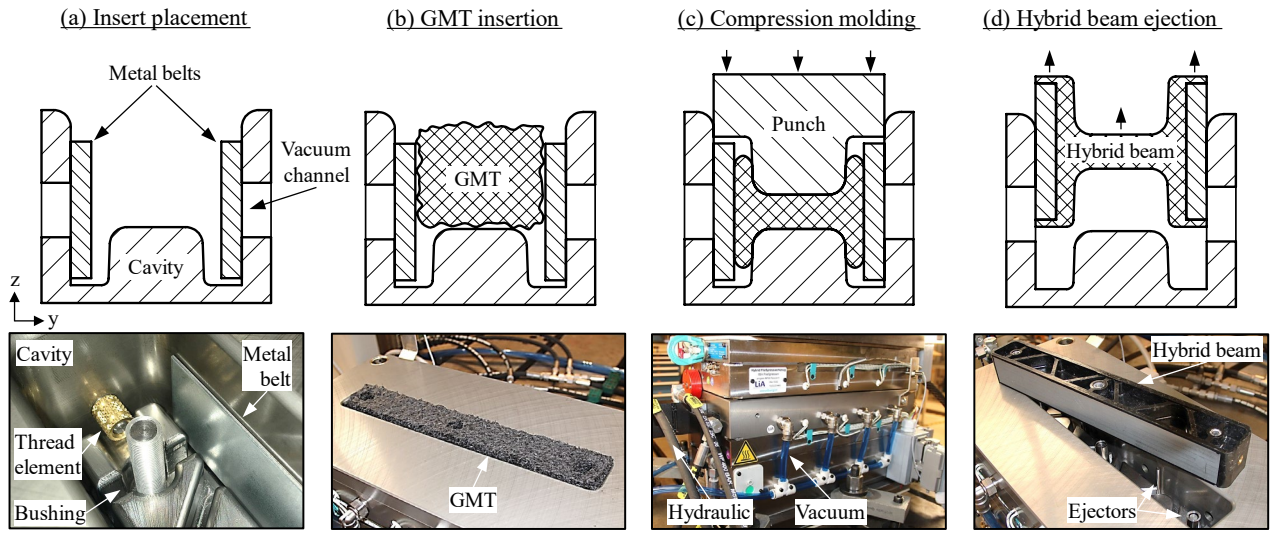

Fig. 1: Process sequence of the innovative molding technology

Process Development

Hybrid beam. For the process development a demonstration part is designed, that consists of outer metal sheets and an inner GMT core structure to propose a lightweight and load adapted hybrid design for bending structures (Fig. 2). The hybrid beam shows typical geometry elements of real applications to reproduce parts' complexity. These include reinforcing ribs and wall thickness variations of the core structure, load introduction elements with and without threads transverse as well as parallel to the direction of press stroke. The optimization potentials resulting from a variable cross-section height and width over the beam length are not considered yet.

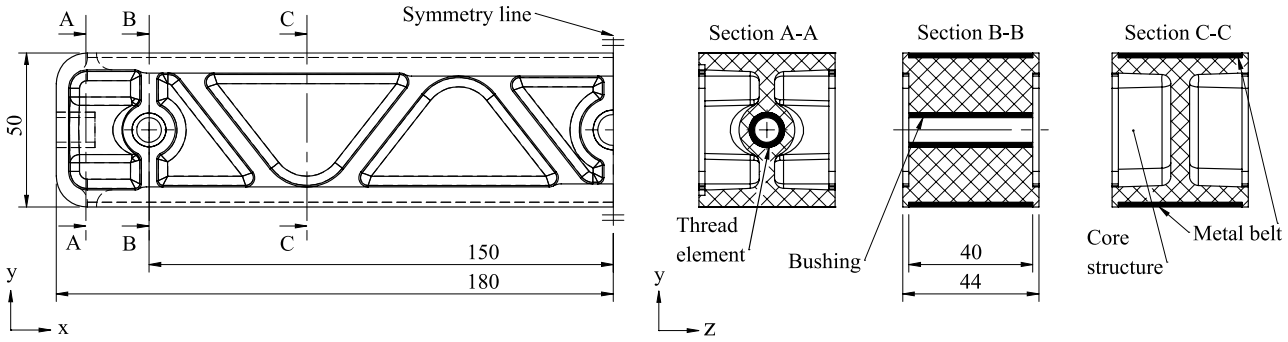

Fig. 2: Design of the demonstration part

The beam length is designed to meet a support distance of 300 mm in a three-point bending load case. The upper and lower metal belts with 340 mm length and 40 mm width extend beyond the support distance. Additional edge areas with a 10 mm fillet on both sides fulfill functional and manufacturing purposes.

The height of the beam was defined to be one sixth of the length to achieve a low shear loading compared to bending. The total width is composed of the width of the metal belt and an edge area for manufacturing reasons. The GMT in the edge area of the metal belt makes the process tolerant to varying amount of material input. This prevents the punch from contacting the metal belts in case of low GMT filling mass, which could cause wear/damage to the tool. In addition, it is ensured that the tools' bottom dead center does not prevent the complete compression of the GMT. With this design, process-side errors can be reduced.

Three bushings are used for the load introduction elements, which are arranged around the neutral fiber of the beam in order to not weaken the highly stressed edge fiber areas. The bushings are surrounded by GMT and embedded directly in the compression molding process. The bushings have

a thread-like structure on the outer shell to achieve a form fit with the GMT. Standard M8-thread elements are inserted into the hybrid beam at the head end and have a knurled surface.

The core structure is designed for the selected load case of three-point bending with the help of a topology optimization. The wall thicknesses vary from 4 to 6 mm and depend on the wall thickness of the metal sheet in the belt area (fewer metal results in more GMT). All forming surfaces parallel to the pressing direction are provided with a demolding bevel of 2°.

Molding tool design. The compression molding tool is made of two halves and each has an electrical temperature control. The ejector system and mandrels for the bushings and thread elements are located in the lower half of the tool. The ejector system consists of pins and sleeves that are hydraulically actuated. The pins are strategically placed to vent the lower half of the mold and the sleeves slide over the core pins onto which the bushings are placed and positioned. The thread elements are held in position by lateral mandrels perpendicular to the stroke direction, which are also hydraulically actuated. The lower mold half is designed as a frame into which the punch of the upper mold half intrudes. The mold frame also serves to position and fix the metal belts. Slippage of the metal belts before and during the compression molding is prevented by a vacuum fixation, which is connected to the metal belt from the outside through four channels on each side. In Fig. 3 a section cut of the closed compression molding tool is shown. The left half of the image shows a central section cut through the core structure and the right half shows a section cut through the metal belt.

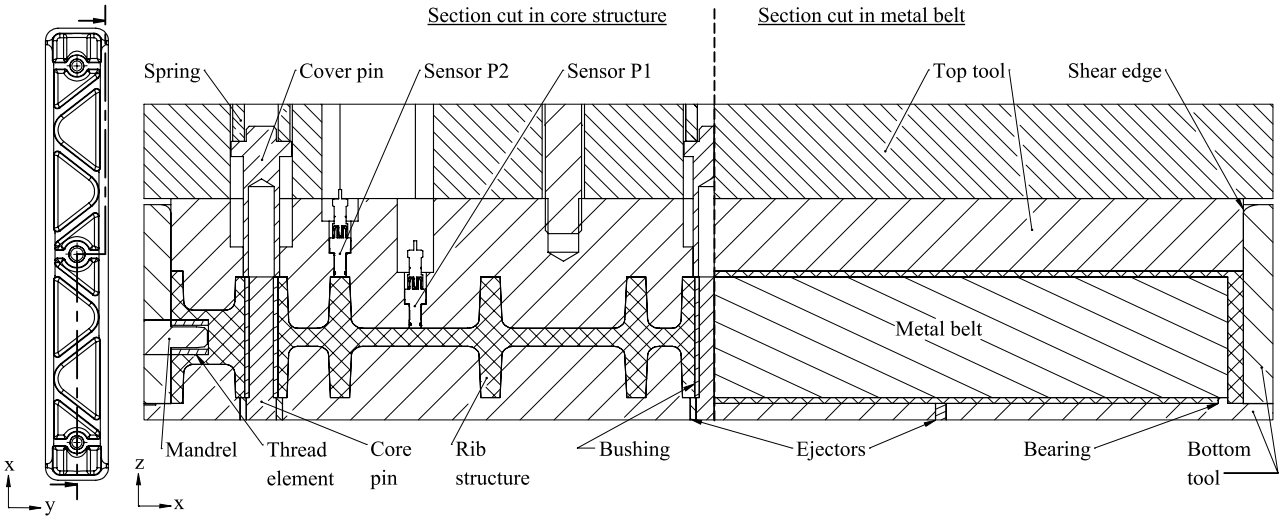

Fig. 3: Section cut of hybrid beam in closed compression molding tool.

The punch of the top tool contains cover pins for the bushings and pressure sensors for process monitoring. The cover pins are pretensioned by compression springs and protrude 25 mm from the mold before the compression molding process starts. When the mold is closed, the cover pins first contact the bushings before the GMT begins to fill the mold. This prevents GMT from flowing over or into the bushings which would require a drilling process afterwards.

The membrane surface of the piezoelectric pressure sensors has a diameter of 4 mm and is aligned perpendicular to the stroke direction. The pressure sensor for pressure measurement P1 is in the lowest position of the punch and thus points on the web area of the core structure. The pressure sensor P2 is in the upper end of an adjacent reinforcing rib for monitoring the mold filling.

Furthermore, the tool is connected to a draw-wire sensor and piezoelectric load cells between the tool and the press to measure the press stroke Z and force K. The measurement is started automatically via an inductive proximity switch, which is triggered by the top tool 35 mm before bottom dead center.

Materials. The material used for the core structure is a commercially available GMT with a fiber content of 52 %, supplied from Mitsubishi Chemical Advanced Materials. The chopped fibers are randomly distributed and embedded in a mineral filled polypropylene (PP) matrix. This material was

chosen due to its good flow properties, homogeneous fiber distribution and high weight specific strength.

The metal belts are made of micro-alloyed steel with zinc coating on both sides HX340LAD +Z100MBO (1.0933) and a thickness of 1.5 mm. In addition, the steel sheet is provided with an adhesive film on one side, which is oriented towards the core structure during the manufacturing process. The PP-based adhesive film is delivered and applied to the steel surface by nolax.

The bushings are made of aluminum alloy EN AW-2007 T4 (AlCu4PbMgMn) and the material for the thread elements is brass. The mechanical properties of the metal belt and core structure materials are presented in Table 1.

Table 1. Material properties of metal belts and core structure

Material	HX340LAD	GMT PP-GF52
Density (g/cm³)	7.85	1.40
Tensile modulus (GPa)	205.00	8.60
Tensile strength (MPa)	448.00	145.00

Process and parameters. The production process is divided into preparation and compression molding. Preparation includes the manufacturing of all semi-finished products, the heating of the GMT blanks and the loading of the compression molding tool with those semi-finished products. The compression molding process consists of the press stroke, the holding time and the opening of the mold with subsequent component ejection.

For preparation, the metal belts are cut to size using a plate shear. The GMT sheets are contoured using water jet cutting. The GMT blanks show the outer contour of the cavity and are cut out at the positions of the three aluminum bushings. In the following, four of the GMT blanks are stacked and weighed to check the right amount of mass. Afterwards they are heated in a convection oven at 250 °C for 10 min. Meanwhile, the functional elements are placed on the holding mandrels and the metal belts are placed and fixed in the mold. A vacuum of -0.8 bar relative pressure is applied for the fixation of the metal belts. The metal belts are heated conductively due to contact with the mold, that is constantly controlled to 100 °C. The temperatures on the coated surfaces of both metal belts are measured with thermocouples (Fig. 4). From the diagram the time interval between inserting the upper and lower metal belts into the cavity can be seen. After 90 s a constant surface temperature of 91.5 °C is reached on the adhesive side of both metal belts.

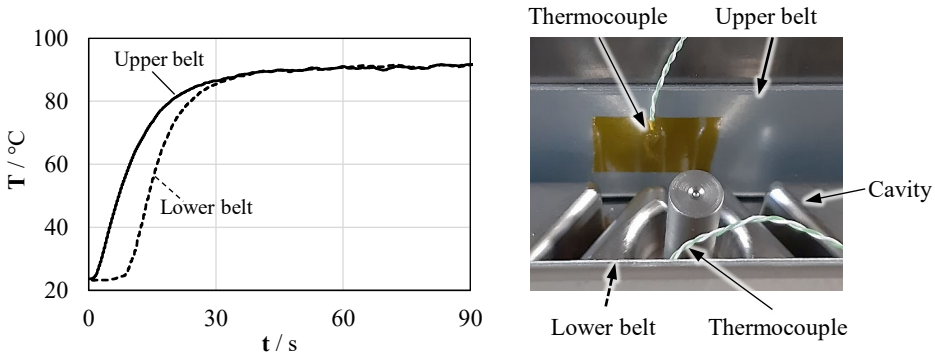

Fig. 4: Measurement of belt temperatures after fixation in molding tool and before insertion of GMT

The compression molding process is executed with a hydraulic press that moves with a speed of approximately 30 mm/s. After inserting the hot and lofted GMT blanks the mold is closed. For 30 s the maximum press force is applied. Afterwards the press stroke is locked for further 30 s. After 60 s in total the mold is opened. Fig. 5 shows the measured process data over time.

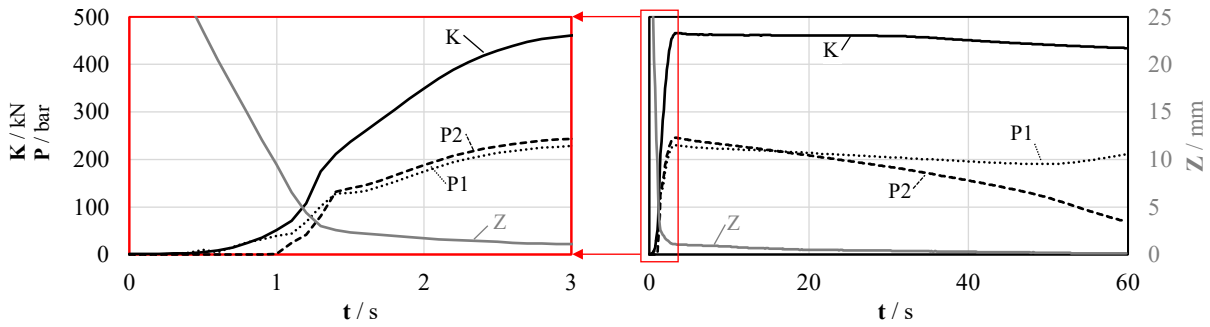

Fig. 5: Measurement of press force K, stroke Z and inner cavity pressures P1, P2. The left diagram shows the process beginning in detail and the right diagram covers the whole cycle time.

The data recording from the beginning of the process shows the flow process and cavity filling. First, the pressure $P1$ increases in the front surface of the punch, which first contacts the lofted GMT. Then the cavity fills and when the GMT reaches the tips of the ribs, the pressure $P2$ increases there as well. During the molding process a maximum force of 467 kN is reached. The maximum pressure $P1$ is 230 bar and the maximum pressure $P2$ is 245 bar. After reaching the peaks both pressures $P1$ and $P2$ drop. Pressure $P2$ drops faster than $P1$ which can be related to the faster cooling and shrinkage of the GMT in the rib area due to higher surface-to-volume ratio. The pressure increase of $P1$ towards the end of the process can be explained by the pressure decrease in the rib areas. While the pressure decreases in some areas (ribs), the pressure outside the ribs must increase to maintain the nearly constant press force.

The initial press speed decreases when the press force increases. The stroke still reduces over the holding and cooling time which can be explained with the shrinkage of the GMT.

Before ejection of the part, the holding mandrels of the thread elements on the top sides of the part are pulled out of the mold to remove the form lock. After ejection and a short cooling time, the hybrid parts are de-burred manually at the ejector points and on the upper outer edge due the closing gap of the tool. Fig. 6 shows a hybrid beam that was manufactured with the one-step compression molding process described above. The hybrid beam is milled on two planes on the left side to visualize the fiber content and orientation.

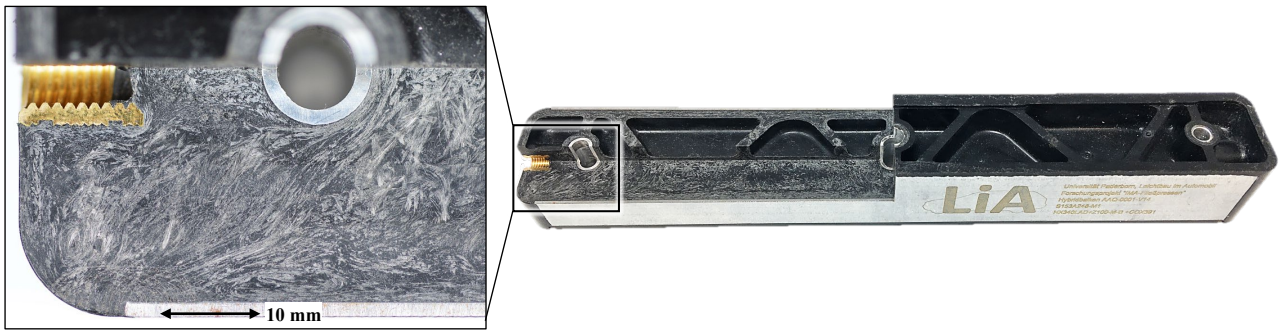

Fig. 6: Manufactured hybrid beam and visualization of fiber content and orientation

By visual inspection, areas of low fiber content cannot be detected neither in the ribs nor in the large area of the bar. The fibers flow around the functional elements and lay down on the surface of the metal belts. Here, the fibers do not show a clear orientation.

Mechanical Testing Results

Testing method. The mechanical characterization of the manufactured hybrid structure is carried out following the procedure of Modler et al. [9] and Fang et al. [10] as well as the norm for characterization of sandwiches [12] in a three-point bending test. The test rig is visualized in Fig. 7.

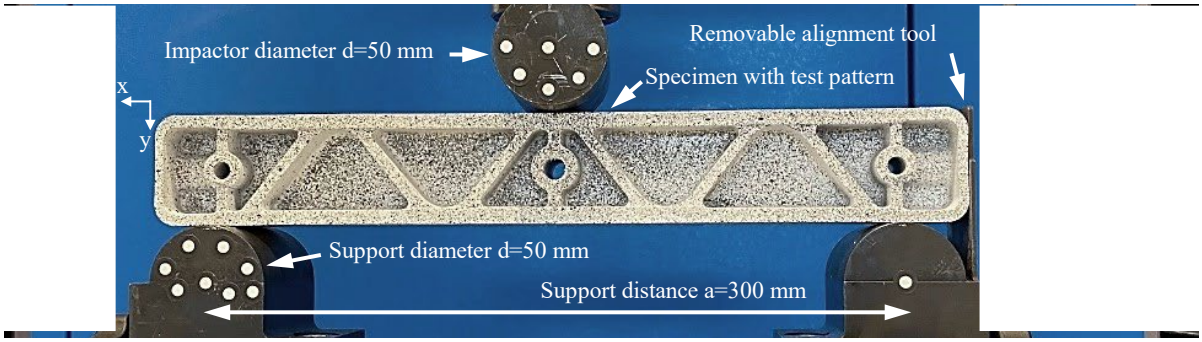

Fig. 7: Test rig for three-point bending

The fixture is driven by a servo-electric universal testing machine with displacement control and a constant traverse speed of 5 mm/min. During the test, the resulting force F on the impactor and the surface displacement $\bar{S}$ of the structure and the test rig are measured optically via digital image correlation (DIC). The vertical relative displacement of the punch to the support points is defined as displacement S. From three-dimensional surface displacement the true strain $\bar{\varepsilon}$ is computed.

Before the test, a stochastic surface pattern is sprayed onto the front and the underside of the hybrid beam to support the DIC. The underside of the beam is optically measured before the test. The hybrid beam is then placed in the fixture. The impactor is contacted with the hybrid beam and the test program as well as the data recording is started. During the test, the frontside of the hybrid beam is optically measured. The test ends at maximum displacement $\hat{S}$ when the force drops to 10 % of the peak force $\hat{F}$. After the end of the test program, the underside of the hybrid beam is measured again to correlate the deformation of the lower belt with the undeformed stage. Thereby, a continuous and a two-stage deformation measurement of the frontside respectively underside of the hybrid beam are available for test evaluation. From force-displacement (F-S) diagram, the fracture energy E

$$E = \int_0^{\hat{S}} F \, dS, \tag{1}$$

the stiffness c

$$c = (F_2 - F_1) \,/\, \big(s(F_2) - s(F_1)\big) \text{ with } F_1 = 0{,}05\ \hat{F} \text{ and } F_2 = 0{,}25\ \hat{F} \tag{2}$$

and the mass-specific energy absorption SEA

$$SEA = E/m \tag{3}$$

are calculated.

Bending properties. In Fig. 8 the resulting F-S curves of two hybrid beams and one GMT-beam without the metal belts are illustrated. The two hybrid beam curves display different test results that were exhibited due to varying manufacturing conditions. The reasons for the different behavior are discussed later. The GMT-beam was manufactured as a reference in the same molding tool, but the vacuum channels were closed as no metal belts were inserted.

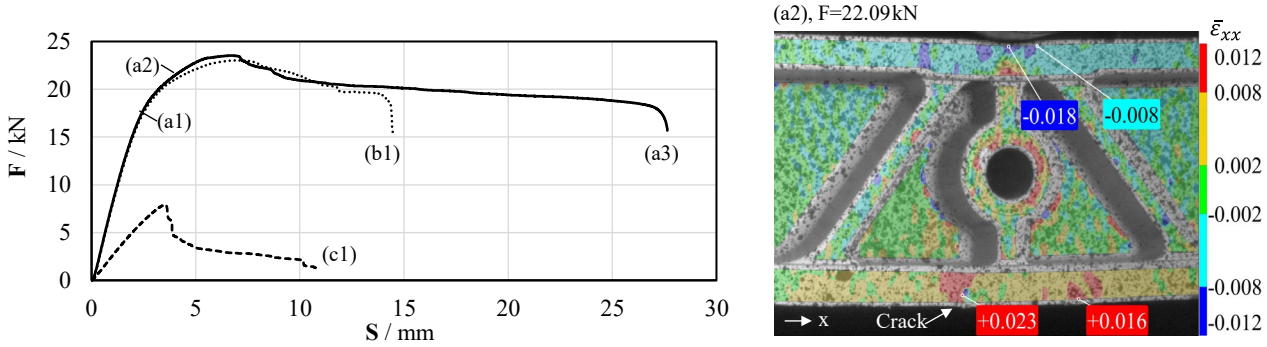

Fig. 8: F-S curves of hybrid beams and contour plot of strain distribution

Curve (a) shows the mechanical behavior of a hybrid beam where the lower belt fractures as intended. At the beginning of the test the force increases linearly until the system stiffness reduces in point (a1). The reduction of system stiffness is correlated to the plasticization of the metal belts. The force increases further and a first crack in the lower, tensile loaded region of the core structure appears (a2). The location of the crack beginning is marked in the DIC-image (Fig. 8, right). After the curves peak, the force drops to a plateau where the force level is nearly constant until the structure completely fails (a3). While the crack in the core structure travels through the vertical rib around the middle bushing, the core still stabilizes the metal belts. The tensile load due to bending is completely transferred by the metal belt in the lower beam region. The whole structure loses mechanical integrity when the lower metal belt fractures.

Curve (b) shows the mechanical behavior of a hybrid beam where the lower metal belt separates from the core structure before fracture. Until the complete failure of the hybrid beam the curves (a) and (b) are similar. When the structure collapses (b1), the lower metal belt delaminates from the core structure in sliding mode two (in-plane shear). The metal belt shows no rupture and is still connected to the core structure from the left end to the middle. Due to the early adhesive failure, the load bearing capacity of the lower metal belt is not completely used.

Curve (c) is from a reference GMT-structure that has no metal belts. The force increases linearly until the maximum (c1). Then, a crack in the lower middle region appears and travels upwards through the beam. The failure appears directly after the peak force. Table 2 lists the characteristic values that can be used to compare the bending properties of the three specimens.

Table 2. Properties of specimens

Specimen	(a) hybrid	(b) hybrid	(c) GMT
$m\ (kg)$	0.79	0.78	0.52
$\hat{F}\ (kN)$	23.52	23.02	7.89
$c\ (kN/mm)$	9.04	8.89	2.70
$E\ (J)$	533.05	279.29	44.24
$SEA\ (J/kg)$	674.75	358.06	85.08

The measurement on the underside of hybrid beam (a) is shown in Fig. 9. The true strain in beam length direction $\bar{\varepsilon}_{xx}$ is analyzed and shown as a contour plot. Furthermore, the strain is evaluated on three sections along the beam axis with a distance of 12.5 mm between the lines.

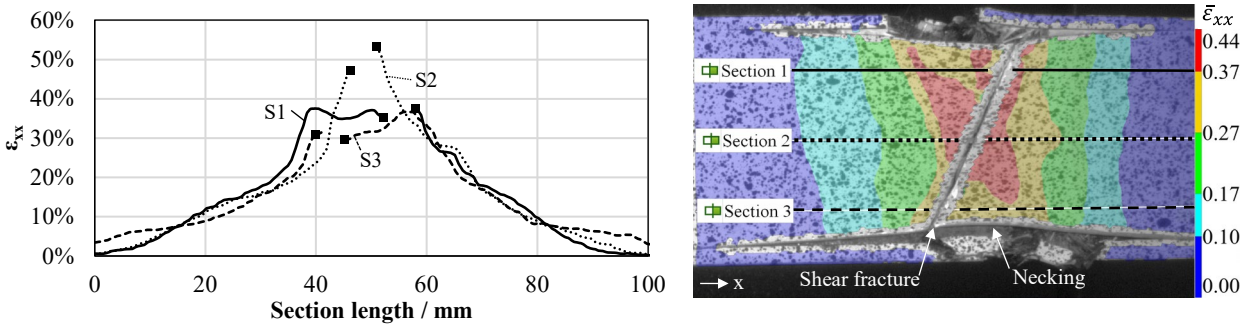

Fig. 9: Strain measurement of lower belt on hybrid beam specimen (a)

A shear fracture in the lower beam as well as the necking region in the middle of the beam length can be obtained from the underside measurement. A shear band with high strain has developed symmetrically to section two (S2) at the same angle of the fracture plane. From the strain measurement curves the local high plasticization of the metal belt can be seen.

Discussion

Process variation. Two hybrid beams have been tested under three-point bending. The hybrid beams were manufactured with the same set-up but showed different mechanical characteristics. The hybrid beam (a) failed as intended due to a crack in the lower metal belt, while in the hybrid beam (b) the metal belt separated prematurely from the core structure. This resulted in the metal belt not transferring the load until failure, and the absorbed energy E of the whole structure (b) was thus less than that of (a). The reason for this different behavior is not clarified yet. The reduced shear strength of the connection between the cover sheet and the core structure could have various causes. First, trapped air could prevent the formation of a material joint. Second, the adhesive film could have been damaged by the GMT insertion and flow process. Another cause could be the premature solidification of the GMT flow front, which does not form a sufficient bond with the adhesive film. Because the manufacturing process is subject to variations due to manual insertion of the plasticized GMT, the bond strength may vary. The cause of insufficient adhesion on some specimens will be clarified in further investigations (e. g. by micrograph analyses) and eliminated by optimizing the manufacturing process.

Comparison of hybrid beam and reference. In comparison to the GMT reference a significant increase in strength, stiffness and energy absorption could be achieved by integration of two metal belts. Due to the two metal belts, the hybrid variant (a) has 52 % more mass than the GMT variant (c). But at the same time, the energy absorption increases by 1105 %. This results in a SEA which is increased by 693 % with the hybrid variant (a) compared to the GMT variant (c).

These advantages are achieved by a high material utilization of the different materials steel and GMT. According to their strengths, the materials are arranged in such a way that they match the different occurring stresses over the beam height. The lightweight and easily formable GMT is placed in the core region, where it has a supporting and functional effect. The metal belts are used in the edge area of the beam, where high normal stresses prevail due to bending. Because of the high yield strength and the broad range of plasticity of the steel, the metal belts can absorb large amounts of deformation energy. Even at the point where cracks are already present in the core structure, the metal belts still transfer the load and provide structural integrity. This can also be evaluated as an excellent fail-safe property, which is necessary for structural and safety-related applications.

Summary

An innovative compression molding technology was developed and experimentally validated for in-mold assembling hybrid structures in bending loaded applications. Using a hybrid beam with two outer metal belts and a GMT core structure as demonstration component, a prototypic tool was developed for analyzing the process and manufacturing specimens. The specimens were characterized

in a three-point bending test. Process-related variations affected the (shear) strength of the adhesive bond between the GMT core structure and the metal belt, resulting in premature delamination of the metal belts from the core structure in one hybrid beam specimen. The causes of this have not been clarified yet and are part of future investigations.

A hybrid beam without process-related defects, in contrast, failed as planned due to cracking of the lower metal belt and exhibited high mechanical properties. Compared to reference beams made only of GMT, a SEA increase of 693 % was achieved with the hybrid variant.

With the aid of the new in-mold assembly technology, a hybrid beam can be manufactured in a single step, combining the forming of the GMT core structure and joining with two outer metal belts. Such lightweight structures could not previously be manufactured in one step, which means that a rational manufacturing process is now available for hybrid bending structures, with which both performance- and cost-driven large series can be addressed.

By selecting different materials for the core and belt structure, various material compatibilities can be investigated for further applications. An additional form closure of the core structure to the metal belts, equivalent to the injection clinching joints by Abibe et al. [13], is a potential optimization strategy to increase the shear strength of the joint and adjust the failure behavior of the whole beam. Furthermore, the variation of the cross-section dimensions over the beam length remains another important variable that can be optimized in the future.

Acknowledgements

This research was supported with grants from the state of North Rhine-Westphalia as part of the "Program for the rational use of energy, regenerative energies and energy saving - progres.nrw-Research program area".

References

[1] B. Bader, W. Berlin, M. Demes, Steigerung der Leichtbaugüte durch interdisziplinäre Zusammenarbeit, Lightweight Des. 12 (2019) 52-57.

[2] D. Drummer et al., Handbuch Kunststoff-Metall-Hybridtechnik, Lehrstuhl für Kunststofftechnik, Erlangen, 2015.

[3] B. Koch, G. Knözinger, T. Pleschke, H.J. Wolf, Hybrid-Frontend als Strukturbauteil, KU Kunststoffe 89 (1999) 82-86.

[4] V. Sellappan, S. Kotrika, G. Arakere, A. Obieglo, M. Erdmann, J. Holzleitner, Suitability analysis of a polymer–metal hybrid technology based on high-strength steels and direct polymer-to-metal adhesion for use in load-bearing automotive body-in-white applications, Journal of Materials Processing Technology 209 (2009) 1877-1890.

[5] G. W. Ehrenstein, S. Amesöder, L. Fernandez, H. Niemann, R. Deventer, Werkstoff- und prozessoptimierte Herstellung flächiger Kunststoff-Kunststoff und Kunststoff-Metall-Verbundbauteile (2003) 149-178.

[6] L. Hoffmann, B. Faißt, K. Kose, F. Eggers, Herstellung und Charakterisierung hochfester Kunststoff-Metall-Hybride, Lightweight Des. 10 (2017) 50-55.

[7] S.-Y. Fu, X. Hu, C.-Y. Yue, Effects of fiber length and orientation distributions on the mechanical properties of short-fiber-reinforced polymers, Materials Science Research International 5 (1999) 74-83.

[8] M. Schemme, LFT-development status and perspectives, Reinforced Plastics 52 (2008) 32-39.

[9] N. Modler et al., Intrinsic Lightweight Steel-Composite Hybrids for Structural Components, Materials Science Forum 825 (2015) 401-408.

[10] X. Fang, T. Kloska, Hybrid forming of sheet metals with long Fiber-reinforced thermoplastics (LFT) by a combined deep drawing and compression molding process, International Journal of Material Forming 13 (2020) 561-575.

[11] D. Heidrich, T. Kloska, X. Fang, Abschlussbericht zum BMBF-Forschungsprojekt MultiForm, Siegener Schriftenreihe Automobiltechnik 3 (2019) 1-86.

[12] DIN 53293:1982-02, Testing of sandwiches; Bending test, Beuth Verlag GmbH, Berlin, 1982.

[13] A.B. Abibe, S.T. Amancio-Filho, J.F. Dos Santos, E. Hage, Development and analysis of a new joining method for polymer-metal hybrid structures, Journal of Thermoplastic Composite Materials 24 (2010) 233-249.